Organic & Biomolecular Chemistry

ROYAL SOCIETY OF CHEMISTRY

PAPER

View Article Online
View Journal | View Issue

Cite this: *Org. Biomol. Chem.*, 2021, **19**, 5595

Regio- and diastereoselective Pd-catalyzed aminochlorocyclization of allylic carbamates: scope, derivatization, and mechanism†‡

Bruna Papa Spadafora, [a] Francisco Wanderson Moreira Ribeiro, [b,c] Jullyane Emi Matsushima, [a] Elaine Miho Ariga, [a] Isaac Omari, [c] Priscila Machado Arruda Soares, [a] Diogo de Oliveira-Silva, [a] Elisângela Vinhato, [a] J. Scott McIndoe, [c] Thiago Carita Correra [b] and Alessandro Rodrigues *[a]

Received 7th April 2021,
Accepted 1st June 2021

DOI: 10.1039/d1ob00670c

rsc.li/obc

The regio- and diastereoselective synthesis of oxazolidinones *via* a Pd-catalyzed vicinal C–N/C–Cl bond-forming reaction from internal alkenes of allylic carbamates is reported. The oxazolidinones are obtained in yields of 44 to 95% with high to excellent diastereoselectivities (from 6 : 1 to >20 : 1 dr) from readily available precursors. This process is scalable, and the products are suitable for the synthesis of useful amino alcohols. A detailed theoretical and experimental mechanistic study was carried out to describe that the reaction proceeds through an *anti*-aminopalladation of the alkene followed by an oxidative C–Pd (II) cleavage with retention of the carbon stereochemistry to yield the major diastereomer. The role of Cu (II) in a C–Cl bond-forming mechanism step has also been proposed.

Introduction

Vicinal difunctionalizations of alkenes under oxidative palladium-catalyzed conditions have emerged as a powerful tool in synthetic organic chemistry.[1] Although there are several recent studies exploring these reactions, they are still much less exploited than the monofunctionalizations of alkenes. This discrepancy can be attributed to the competing β-hydride elimination reaction from Pd(II)–carbon intermediates, complicating the installation of the second functional group. Strategies to overcome this challenge include the use of appropriate oxidants able to drive reductive elimination from Pd resulting in a new adjacent functionalization.[2] These difunctionalization strategies have also been shown to occur with high diastereoselectivities and the stereochemical relationship between the two added groups usually furnishes valuable structural information for mechanistic proposals.[2k,3,4] Examples of intramolecular alkene difunctionalizations *via* aminopalladation include aminoacetoxylation,[2a,5] amino-hydroxylation,[6] amino-fluorination,[7] aminotrifluoro-methoxylation,[8] aminoalkylation,[9] aminocarbonylation,[10] diamination,[2d,3,11] aminobromination[12] and aminochlorination[12a,13] reactions. In this context, allyl carbamates are versatile compounds with considerable potential for the synthesis of valuable building blocks through metal-catalyzed-difunctionalization reactions.

Previous works involving the aminometallation of allylic carbamates and related compounds for the synthesis of oxazolidinones, lactams, and urea, resulting in vicinal nitrogen and chlorine groups, have been reported (Scheme 1a–c). Bach successfully disclosed the Fe(II)-catalyzed radical aminochlorination of a series of alkenes (Scheme 1a, left).[14] In 2015, Xu described an enantioselective Fe(II)-catalyzed aminochlorination of hydroxylamine derivatives (Scheme 1a, right).[15] Recently, Xu reported the $CuCl_2$ mediated aminochlorination reaction of allylic carbamates and related compounds (Scheme 1b).[16] Lu reported one of the first studies involving the intramolecular aminochlorination of olefins catalyzed by Pd(II) (Scheme 1c, left).[13a] Christie demonstrated the crucial role of oxidants in combination with Pd(II) (Scheme 1c, right),[13d] reporting the production of oxazolidinones from allylic carbamates using a combination of Pd(II) and Cu(II). When Cu(II) is absent, a formal [3,3]-sigmatropic rearrangement takes place to produce allylic amides. Despite these successes, the palladium-catalyzed difunctionalization of 1,2-disubstituted alkenes is known to be difficult and current amino-

[a]*Department of Chemistry, Federal University of Sao Paulo, UNIFESP. Prof. Artur Riedel Street 275, lab 10, 09972-270 Diadema, SP, Brazil.*
E-mail: alessandro.rodrigues@unifesp.br
[b]*Department of Fundamental Chemistry, Institute of Chemistry, University of Sao Paulo, Av. Prof. Lineu Prestes, 748, 05508-000 Sao Paulo, SP, Brazil*
[c]*Department of Chemistry, University of Victoria, P. O. Box 3065, Victoria, BC V8W 3V6, Canada*

†Dedicated to Professor Paulo R. Olivato on the occasion of his 50th anniversary as a Professor at the Institute of Chemistry of University of Sao Paulo.

‡Electronic supplementary information (ESI) available. See DOI: 10.1039/d1ob00670c

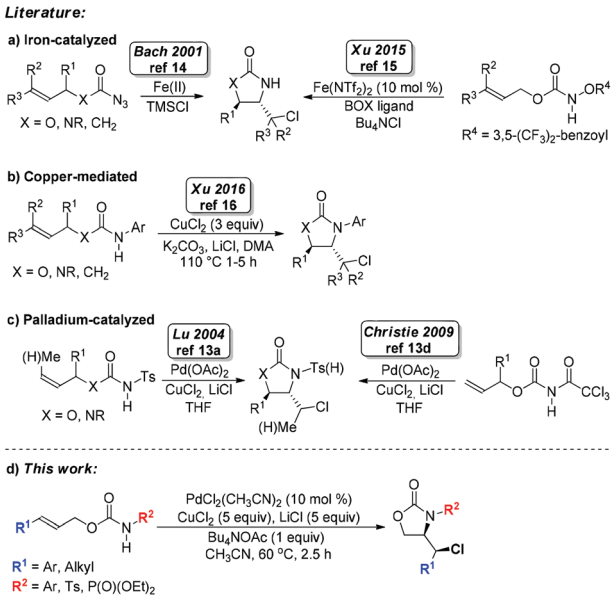

Scheme 1 Context of the work.

chlorination methods generally suffer from limited substrate scope, as many of the reported methods are restricted to terminal alkenes.

This limitation prompted us to develop a method for the Pd-catalyzed aminochlorocyclization of allylic carbamates with internal alkenes (Scheme 1d). We also report additional features of this transformation, such as its scalability, its potential for further derivatization, and experimental and theoretical mechanistic considerations.

Results and discussion

Experimental studies

As the starting point, we chose cinnamyl alcohol-derived carbamate **1a** as a model compound,[17] and it was used to optimize the reaction conditions for the vicinal aminochlorocyclization. The influence of the Pd source, equivalents of oxidant and solvent nature were investigated (Table 1).

Treatment of carbamate **1a** with $Pd(OAc)_2$ (10 mol%), $CuCl_2$ (2 equiv.), LiCl (5 equiv.), and Bu_4NOAc (1 equiv.) in CH_3CN at 25 °C (Table 1, entry 1) was unsuccessful. However, when the reaction was conducted at 60 °C, the ^1H NMR conversion was 74%, and the ratio between the desired oxazolidinone **2a** and decarboxylated aza-Claisen[18] by-product **3a** was 40 : 60 (entry 2). Increasing the amount of the oxidant ($CuCl_2$) up to 5.0 equiv. improved the conversion to 91% and the **2a** : **3a** ratio to 83 : 17 (Table 1, entry 5). Furthermore, various Pd sources were investigated, and no significantly different results were observed, except for $PdCl_2(PPh_3)_2$, which required 12 h to reach 75% conversion and provided a 100 : 0 **2a** : **3a** ratio (Table 1, entry 7). We also explored the effect of various other solvents, such as THF, toluene, CH_2Cl_2, hexane, MeOH and DMSO (entries 10–15); however, CH_3CN remained the most

Table 1 Optimization of aminochlorination conditions[a]

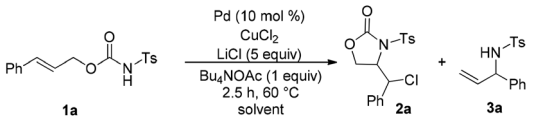

Entry	Pd	Solvent	$CuCl_2$ (equiv.)	Convn[b] (%)	**2a** : **3a**[c]
1[d]	$Pd(OAc)_2$	CH_3CN	2	0	—
2	$Pd(OAc)_2$	CH_3CN	2	74	40 : 60
3	$Pd(OAc)_2$	CH_3CN	3	80	87 : 13
4	$Pd(OAc)_2$	CH_3CN	4	90	83 : 17
5	$Pd(OAc)_2$	CH_3CN	5	91	83 : 17
6	$Pd(TFA)_2$	CH_3CN	5	86	83 : 17
7	$PdCl_2(PPh_3)_2$	CH_3CN	5	61(75)[e]	100 : 0
8	$PdCl_2$	CH_3CN	5	90	84 : 16
9	$PdCl_2(CH_3CN)_2$	CH_3CN	5	92	86 : 14
10	$PdCl_2(CH_3CN)_2$	THF	5	84	81 : 19
11	$PdCl_2(CH_3CN)_2$	$PhCH_3$	5	73	77 : 23
12	$PdCl_2(CH_3CN)_2$	CH_2Cl_2	5	71	66 : 34
13	$PdCl_2(CH_3CN)_2$	Hexane	5	82	77 : 23
14	$PdCl_2(CH_3CN)_2$	MeOH	5	23	100 : 0
15	$PdCl_2(CH_3CN)_2$	DMSO	5	49	86 : 14

[a] Reaction conditions: **1a** (0.2 mmol), solvent (0.1 M). [b] Conversion of a mixture of **2a** and **3a** determined by ^1H NMR spectroscopy of the crude reaction mixtures. [c] Product distribution determined by ^1H NMR spectroscopy of the crude reaction mixtures. [d] 25 °C, 7 h. [e] 12 h.

efficient solvent (entry 9), promoting a high **2a** : **3a** ratio of 86 : 14.[19] Control experiments[20] indicated that no aminochlorocyclization occurred in the absence of palladium or lithium chloride. Moreover, in the absence of $CuCl_2$, only allyl sulfonamide **3a** was formed in 87% and 40% conversion using 10 and 100 mol% of $PdCl_2(CH_3CN)_2$, respectively. The use of 1.0 equiv. of Bu_4NOAc was crucial for generating product **2a** in higher yield.

Conducting the reaction in the absence of Bu_4NOAc resulted in a 66 : 33 ratio of products **2a** and **3a** in only 15% conversion.[20] The reaction was neither moisture- nor air-sensitive, and the results were reproducible using unpurified commercial solvents.

Once we identified conditions that provided satisfactory results for the aminochlorocyclization of **1a** (Table 1, entry 9), we began to explore the reaction scope (Scheme 2). First, various tosylcarbamates (**1a–l**) with terminal aryl moieties were surveyed. Substrate **1a** afforded product **2a** in 65% yield with excellent diastereoselectivity (20 : 1). Electron-donating substituents such as –OMe (**1b–d**) and –Me (**1e**) gave similar results with slightly reduced yield and diastereoselectivities when compared to substrate **1a**. Conversely, substrates bearing benzene rings with electron-withdrawing substituents such as nitro (**1h** and **1i**) offered improved yields and diastereoselectivities, furnishing **2h** and **2i** in 70% (dr >20 : 1) and 60% (dr >20 : 1) yields, respectively.

Despite this, chlorinated substrate **1j** furnished product **2j** in 60% yield and only 6 : 1 dr. Fused bicyclic **2f** was obtained in a moderate yield with excellent diastereoselectivity (>20 : 1). Notably, a substrate bearing an α-naphthyl group afforded the desired product (**2g**) in excellent yield (92%) and diastereo-

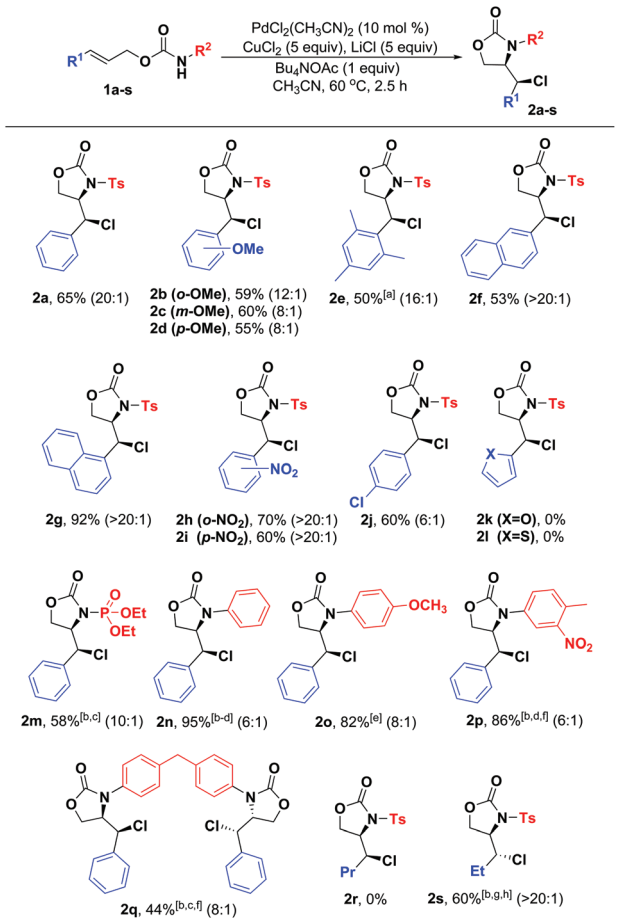

Scheme 2 Scope of the reaction – variation of R^1 and R^2: effect on yields and diastereomeric ratio. Reaction conditions: **1a–q** (0.2 mmol), $PdCl_2(CH_3CN)_2$ (0.02 mmol), $CuCl_2$ (1.0 mmol), LiCl (1.0 mmol), Bu_4NOAc (0.2 mmol), CH_3CN (0.1 M). Yields are isolated yields (average of three experiments). The data in parentheses are the diastereomeric ratio (dr) determined by ^1H NMR analysis of the crude reaction mixture. [a] At 50 °C. [b] For 24 h. [c] Bu_4NOAc (0.4 mmol). [d] At 80 °C. [e] For 5 h. [f] Solvent mixture (CH_3CN : THF 1 : 1). [g] At 25 °C. [h] From *Z*-isomer.

selectivity (>20 : 1). On the other hand, furan **1k** and thiophene **1l** are not compatible substrates with the reaction conditions, and only traces of the desired products were detected along with many by-products. The formation of these by-products could be attributed to the low stability of compounds **1k** and **1l**, which must be used without further purification. Moreover, nontosyl carbamates bearing other groups on the nitrogen atom, such as diethoxyphosphoryl or aryl (**1m–q**), were also suitable for the reaction, although some of the standard reaction conditions had to be altered.

In order to expand the scope to the aliphatic substituted alkenes, we selected the derivatives (*E*)-**1r** and (*Z*)-**1s**. Only traces of product **2r** were detected by ^1H NMR from terminal propyl derivative **1r**. Under the optimized methodology, (*E*)-**1r** alkyl derivative proved to be a poor substrate for aminochlorocyclization and to favor formal [3,3]-sigmatropic rearrangement[18] which was obtained in 23% yield. The heterocycle **2s** was obtained in 60% yield from (*Z*)-ethyl derivative **1s**.

This result is consistent to that obtained by Lu[13a] for the corresponding (*Z*)-methyl terminal allylic tosyl-carbamate. The relative stereochemistry of **2o** was determined by comparison of the experimental NMR data for the same compound described by Xu and co-workers.[16] The relative stereochemistry of **2a** was determined by full NMR analysis and the relative stereochemistry of the other oxazolidinones were proposed by analogy based on the NMR patterns of compounds **2a** and **2o**. Remarkably, all ring-forming allyl alcohol derivatives **2a–s** underwent 5-*exo*-closure to generate one regioisomer under the optimized conditions, which shows the excellent regioselectivity of the palladium-catalyzed reaction.[13a,21]

To test the practicality of our methodology, two reactions on gram-scale were carried out using substrate **1a** (Scheme 3). Product **2a** was obtained with results comparable to those of the 0.2 mmol scale reactions (65% yield, dr 20 : 1). When the reaction was conducted for 24 h using 5 mol% of $PdCl_2(CH_3CN)_2$, the isolated yield improved to 75%.

To demonstrate the synthetic utility of the present methodology, four reactions aiming to synthesize different amino alcohols were carried out (Scheme 4).[22] Heating oxazolidinone **2a** under basic (KOH 0.5 M) conditions generated amino dialcohol **4a** in 66% yield. Treating **2a** with K_2CO_3 in MeOH afforded amino alcohol **5a** in 90% yield. Compounds **4a** and **5a** were likely formed through an aziridine intermediate in a fashion similar to that reported by Shi for an analogous transformation.[23] Oxazolidinone **2a** was subjected to reductive conditions with $LiAlH_4$ or DIBAL-H and furnished compounds **6a** and **7a** in 56% and 57% yields, respectively. The diastereomeric ratios of derivatives **4a**, **5a** and **7a** were maintained at the same level of compound **2a**.

Mechanistic studies

To allow a detailed description of the Pd-catalyzed aminochlorocyclization reaction, a series of experiments and theoretical modelling was carried out. The results are presented in five distinct sections discussing: (i) a set of initial mechanistic hypotheses; (ii) the role of Bu_4NOAc in the initial *anti*-AP and

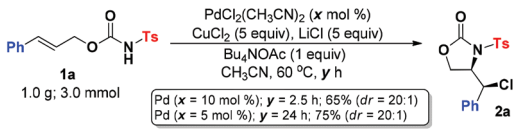

Scheme 3 Chloroaminocyclization on a gram-scale synthesis.

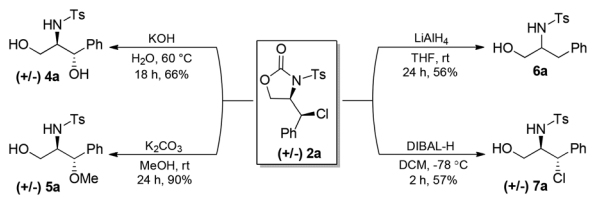

Scheme 4 Synthetic transformations of oxazolidinone **2a**.

syn-AP steps; (iii) the chlorofunctionalization step; (iv) ESI-MS/MS real time evaluation of intermediates; and (v) the consolidated mechanistic proposal.

Mechanistic hypothesis

A set of mechanistic hypotheses involving four main steps for the investigated reaction is depicted in Scheme 5. The formation of the major diastereomer of heterocycles **2** from carbamate **1** indicates an *anti*-addition relationship of the nitrogen from the tosylcarbamate and the chloride to the alkene. This stereochemical outcome has distinct pathways that can be triggered by either an *anti*-aminopalladation (*anti*-AP) **I** and *syn*-aminopalladation (*syn*-AP) **V**, to form the intermediates **II** and **VI**, respectively (Scheme 5). These pathways (*anti*-AP and *syn*-AP) were proposed originally by Henry[24] and supported by other researchers.[2d,3a,25]

Control experiments[20] showed that in the absence of $CuCl_2$, only allyl sulfonamide **3a** was formed *via* a formal [3,3]-sigmatropic rearrangement from carbamate **1a**. The only product was **3a** even when a stoichiometric reaction with Pd(II) is carried out, corroborating the role of $CuCl_2$ in an oxidative mechanism and discarding a Pd(II)/Pd(0) catalysis. Considering the formation of the product **2e** from the tri-substituted allyl carbamate **1e**, we also discarded a mechanism that could involve the formation of an intermediary through a η^3-allylaryl-Pd complex[26] with dearomatization of the arene that should be precluded by the methyl substituents at 2- and 6-phenyl positions. Thus, to incorporate the second functionalization, the intermediates **II** and **VI** could undergo $CuCl_2$ insertion to form **III** and **VII**, respectively, through a heterobimetallic σ-Pd/Cu complex[27] or a transient palladium oxidation, similarly to that postulated by Henry.[28] In the following mechanism step, copper chloride would assists the chlorine transfer from palladium to carbon, to form both major and minor diastereomer of **2**, by *path a* and *d*, respectively. In this mechanistic model, the oxidation state of the palladium remains +2 throughout the process. Alternative mechanisms, which involve the oxidation of Pd(II) to Pd(IV), to form intermediates **IV** and **VIII**, from intermediates **II** and **VI**, respectively, can also be considered (Scheme 5) as the formation of these Pd(IV) intermediates promoted by $CuCl_2$ have been proposed by Chemler,[12a] Perumal,[29] Sridharan,[2l] Shi,[30] and others. The following functionalization step would involve the C–Cl bond formation, that can be reached by a reductive C–Pd(IV) cleavage with retention of the carbon stereochemistry on **IV** by *path a* to form the major diastereomer or *path d* on **VIII** for the minor diastereomer (Scheme 5). Moreover, the C–Cl bond formation could also result *via* an S_N2-type reaction at the palladated carbon of **IV** by *path c* to form the major diastereomer or *path b* on **VI** for the minor diastereomer (Scheme 5). The combination of these mechanistic sequences is grounded on earlier studies developed by Muñiz,[1a] Stahl,[1b] Chemler,[1c,12a] Bäckvall,[1e] Liu,[1f,2c,j,6,13a] Michael,[2d,3b] Sigman[3c] and others.

The role of Bu_4NOAc

To evaluate the proposed mechanistic pathways for this transformation at the molecular level, the steps depicted in Scheme 5 (R^1 = Ph and R^2 = Ts) were modelled by DFT calculations at the M06-2X/Def2-TZVPP(Pd,Cu)/6-311++g(2df,2pd) (all others)//PBE1PBE/Def2-TZVPP(Pd,Cu)/6-31g(d,p)(all others)/SMD level in acetonitrile.[31] Initially, the base Bu_4NOAc was not considered in our calculations for an *anti*-aminopalladation mechanism (Fig. 1).[2a,13a] Carbamate **1a** (model substrate) coordinates to Pd(II) by dissociative substitution of one LiCl from $Li_2[PdCl_4]$ (formed *in situ*),[32] leading to intermediate **Int-A** (analogous to species **I**, Scheme 5), calculated to be 17.5 kcal mol^{-1} in relation to the isolated reactants (Fig. 1). Intermediate **Int-A** then undergoes *anti*-aminopalladation *via* transition state $\mathbf{TS_{AB}}$ with an energy barrier of 35.8 kcal mol^{-1} to form zwitterionic intermediate **Int-B** (analogous to species **II**, Scheme 5) 11.3 kcal mol^{-1} higher in free energy than **Int-A**. This barrier is too high for the aminopalladation to occur in absence of Bu_4NOAc.[1g,3,4]

To survey the role of Bu_4NOAc and to obtain further experimental mechanistic evidence of the palladium-carbamate intermediate formation, titration experiments were carried out and followed by ^1H NMR (Fig. 2). The titration of a CD_3CN solution of **1a** with $PdCl_2(CH_3CN)_2$ up to 1 : 1 equivalent did not result in any change in the NMR signals of carbamate **1a** and the resulting mixture was used to a reference spectrum (bottom of Fig. 2) for the following ^1H NMR experiments. Conversely, the titration of a 1 : 1 mixture of **1a** and $PdCl_2(CH_3CN)_2$ up to an equimolar amount of Bu_4NOAc led to a gradual formation of at least two new sets of signals that could be attributed to intermediates **Int-C** and **Int-G** (Fig. 3) species, which the appearance of new peaks from 6.3 to 7.0 ppm can be ascribed to the alkene entering the coordination sphere of the palladium. This result can justify the role of the base Bu_4NOAc associated with the acidic *N*-tosyl-carbamate **1a** (pK_a = *ca.* 3.7).[33]

Therefore, the mechanistic proposals were reinvestigated considering the involvement of tetrabutylammonium acetate.

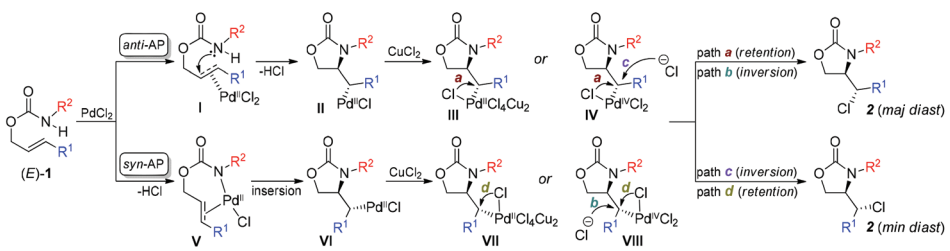

Scheme 5 Mechanistic steps proposed for the amino-chloro-difunctionalization of allylic carbamates **1**.

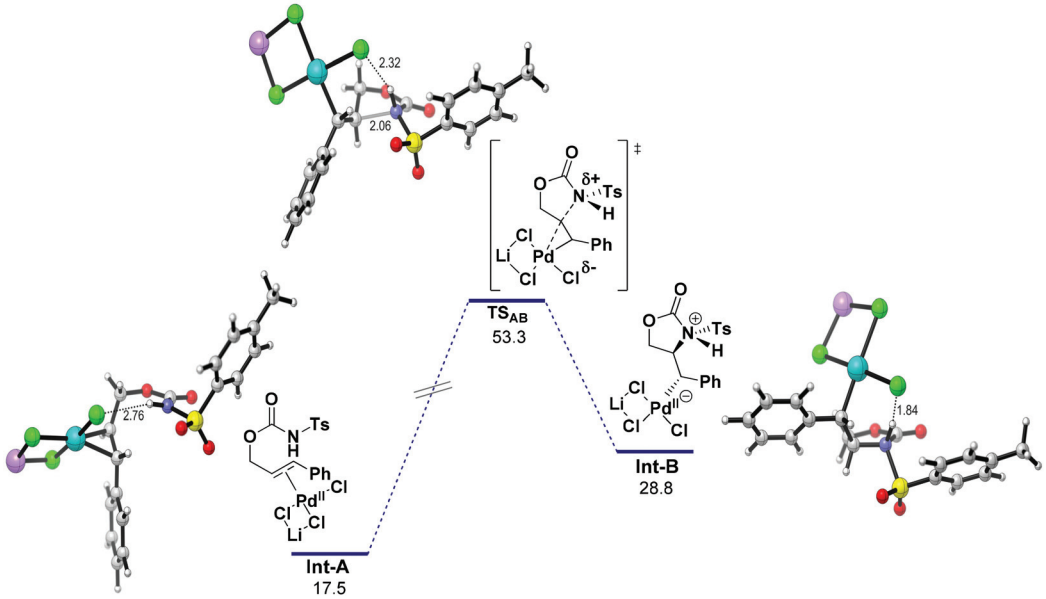

Fig. 1 Computed[31] free energy profile for the neutral *anti*-aminopalladation step of **1a**. ΔG values in kcal mol^{-1} in relation to the isolated reactants (acetonitrile, 333.15 K, 1 atm).

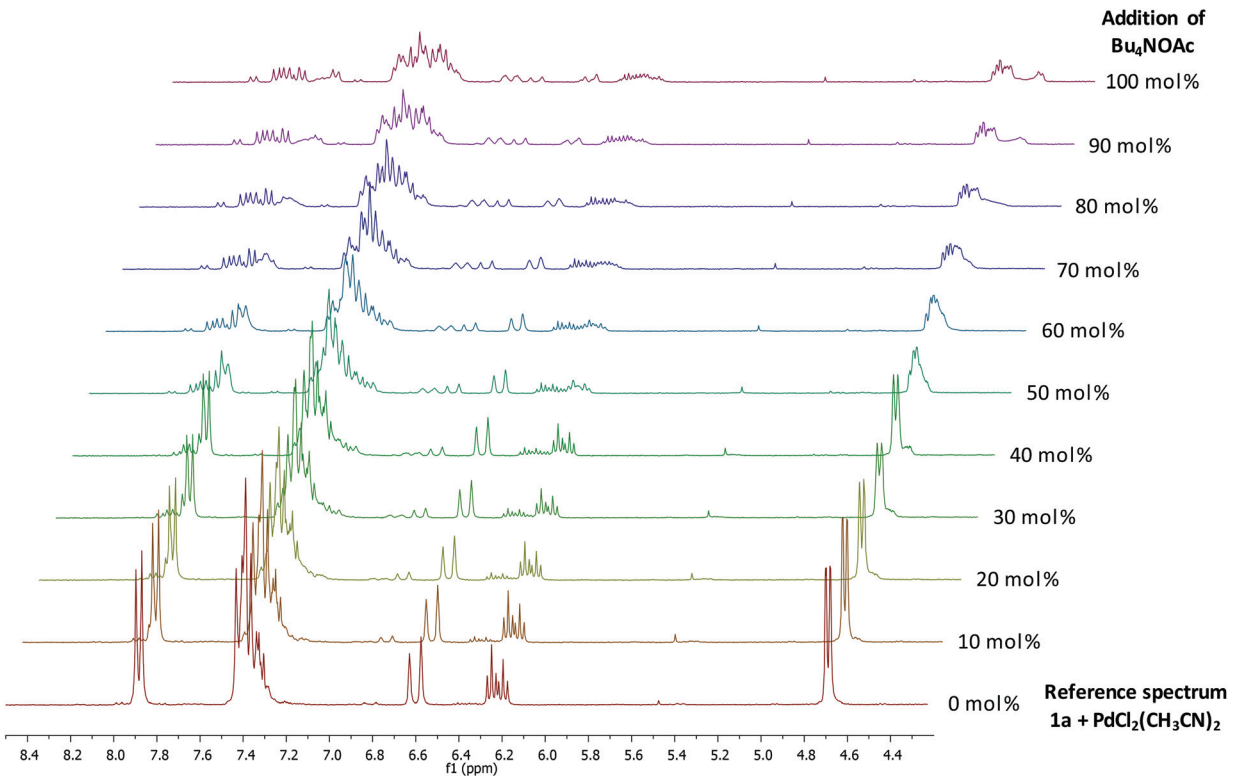

Fig. 2 ^{1}H NMR titration experiments (300 MHz at 25 °C) of a 1 : 1 equivalent mixture of **1a** and $PdCl_2(CH_3CN)_2$ with gradual increasing of Bu_4NOAc concentration.

To reduce computational cost, the experimental tetrabutylammonium ion was replaced by the smaller cationic tetramethylammonium (TMA) species. Inclusion of the tetramethylammonium acetate allowed the computational modelling of the competitive *anti*- and *syn*-aminopalladation steps to form the intermediates **Int-E** and **Int-I**, respectively (Fig. 3) to account for the experimentally observed stereochemical outcome. The *anti*-AP starts with intermediate **Int-C**, which is

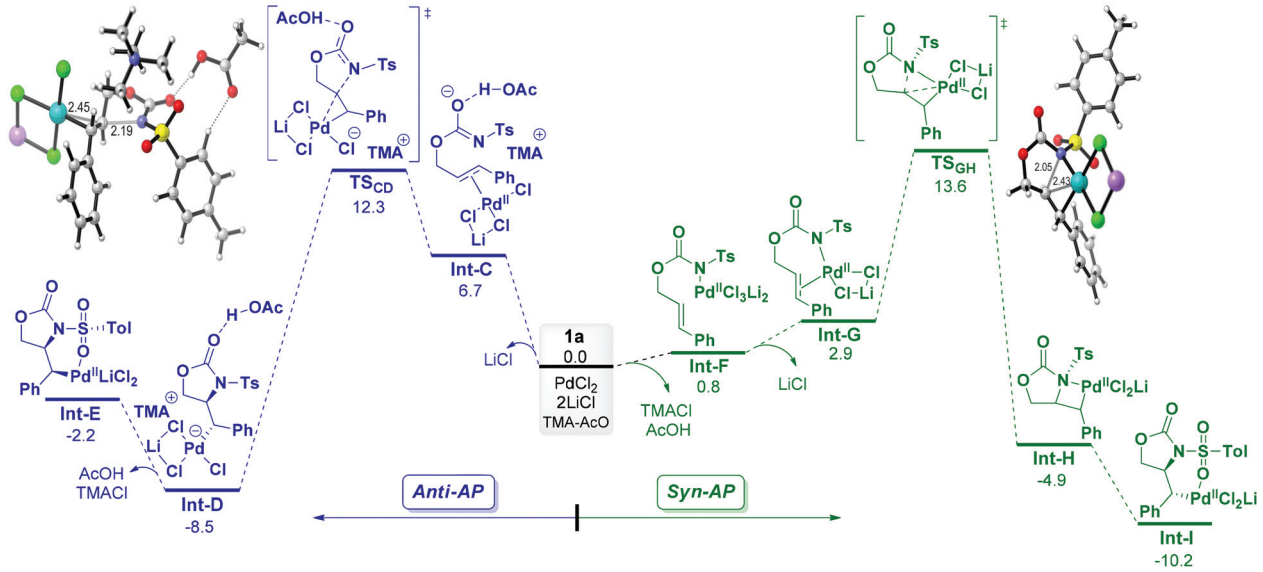

Fig. 3 Computed[31] free energy profile for the *anti*-AP *vs. syn*-AP step of **1a**. ΔG values in kcal mol^{-1} (acetonitrile, 333.15 K, 1 atm).

stabilized by TMA-AcO when compared to the TMA free intermediate **Int-A** (17.5 kcal mol^{-1}, Fig. 1). **C** then proceeds through transition state $\mathbf{TS_{CD}}$ with a barrier of 5.6 kcal mol^{-1} to form a C–N bond *via anti*-aminopalladation, leading to intermediate **Int-D** (−8.5 kcal mol^{-1}). Intermediate **Int-D** releases AcOH and TMA-Cl to afford intermediate **Int-E** (−2.2 kcal mol^{-1}). In the mechanism involving *syn*-AP (Fig. 3), the nitrogen atom of carbamate **1a** is deprotonated and then coordinates to the palladium center of Li_2PdCl_4, releasing one of the Cl^- ligands to give intermediate **Int-F**. Intermediate **Int-F** is easily converted to amidate-alkene chelate **Int-G**, liberating lithium chloride. The next stage includes the formation of metallabicyclic **Int-H** *via* $\mathbf{TS_{GH}}$ for C–N bond formation. Alkene insertion into the Pd–N bond exhibits a barrier of 10.7 kcal mol^{-1}. Intermediate **Int-H** easily undergoes cleavage of the Pd–N bond, forming the six-membered intermediate **Int-I** with a sulfuryl oxygen atom coordinated to the Pd(II) center (Fig. 3). These results suggest that the *anti*-AP pathway is favored over the *syn*-AP pathway ($\Delta G^{\ddagger}$ 12.3 *vs.* 13.6 kcal mol^{-1}). In addition, our calculations agree with the experimental studies on Wacker reactions developed by Bäckvall,[34] Henry,[35] Oxgaard and Goddard III,[36] that suggest the *anti*-AP is a dominant mechanism step when the reaction is conducted at high [Cl^-] and [$CuCl_2$] concentrations.

Chlorofunctionalization step mechanism

Once the initial species involved in the *anti*-AP and *syn*-AP steps were established (Fig. 3), we turned our attention to calculate the next mechanistic intermediates for the chlorofunctionalization. We first developed a mechanistic model in which the oxidation state of palladium remains +2 throughout the process (Fig. 4). Thus, the first-formed σ-alkylpalladium complex intermediates **Int-E** and **Int-I** that resulted from *anti*-AP and *syn*-AP, undergo insertion of 2 equiv. of $CuCl_2$ to form exergonically the heterobimetallic Pd/Cu intermediates **Int-J** and **Int-L**, respectively. The Pd–Cu bimetallic complex with a bridging chloride ligand is proposed based on Hosokawa studies.[37] Next, chlorine transfer from palladium assisted by Cu(II) occurs by forming the C–Cl bond with retention of the carbon configuration, resulting in the palladated intermediates **Int-K** and **Int-M**. Oxidative cleavage of C–Pd bonds by $CuCl_2$ with retention at the carbon atom, in the presence of a large excess of chloride ion, was also observed by Lu and co-workers.[38] The formation of intermediates **Int-K** and **Int-M** occurs *via* cyclic transition states $\mathbf{TS_{JK}}$ and $\mathbf{TS_{LM}}$, requiring an activation free energy of only 3.3 kcal mol^{-1} and 0.7 kcal mol^{-1}, respectively (Fig. 4), in a similar model described by Liu and co-workers[2c,j] and others. The last step involves the dissociative substitution of a coordinated sulfonyl oxygen on palladium of intermediates **Int-K** and **Int-M** by lithium chloride, which regenerates the catalyst releasing major and minor diastereomers of **2a**, respectively.

According to the proposed mechanistic pathways in Scheme 5, an alternative step includes the oxidation of **Int-E** (formed by *anti*-AP mechanism, Fig. 3) to give alkyl Pd(IV) intermediate **Int-N** in the presence of the $CuCl_2$ which is computationally viable (Fig. 5). Although the oxidation of C–Pd(II) to C–Pd(IV) intermediates promoted by Cu(II) salts has been suggested by other authors, there is still a lack of clear evidence to support this hypothesis.

Nevertheless, this proposal cannot be completely discarded. It should be noted that other oxidizing systems, such as H_2O_2/LiCl,[2c] $H_2O_2/CaCl_2$,[2j] could follow this mechanism proposal. A direct reductive elimination from Pd(IV)-intermediate **Int-N** could occur *via* $\mathbf{TS_{NO}}$, forming the C–Cl bond with retention of the carbon configuration. Finally, the main diastereomer of **2a** is formed by dissociative substitution of a coordinated sulfonyl oxygen on palladium by lithium chloride, which regenerates

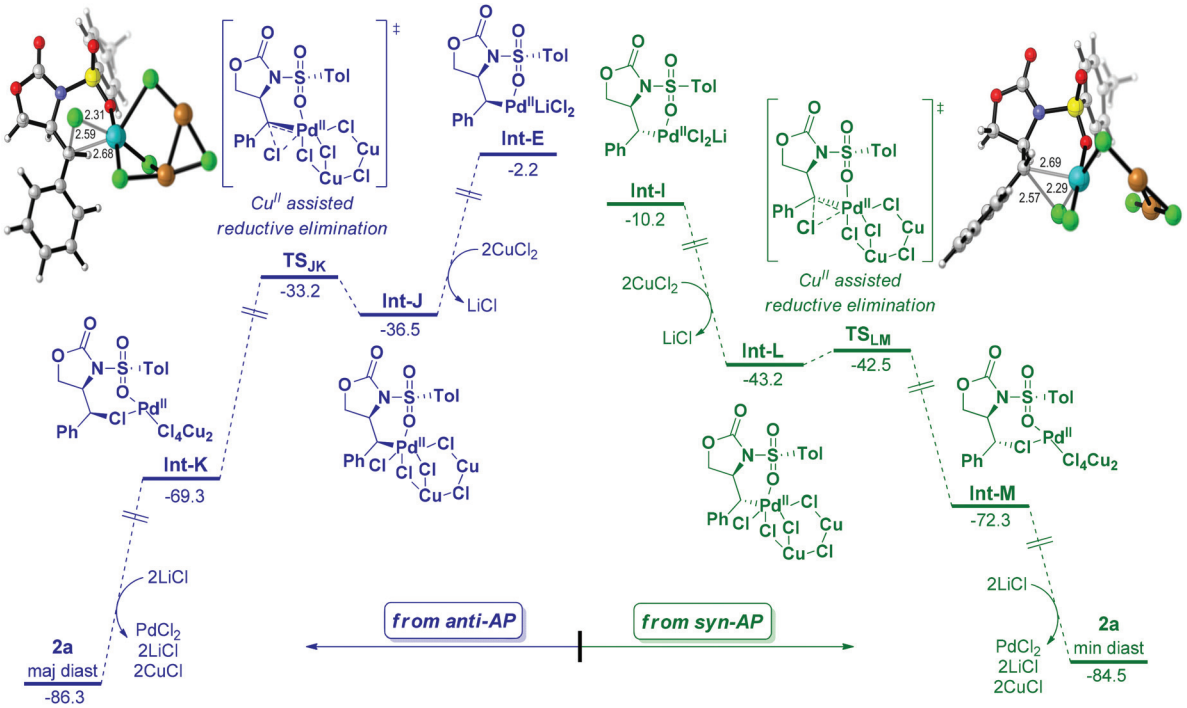

Fig. 4 Computed[31] free energy profiles for the C–Pd reductive elimination step assisted by $CuCl_2$ to the formation of **2a** (both major and minor diastereomers). ΔG values in kcal mol^{-1} (acetonitrile, 333.15 K, 1 atm).

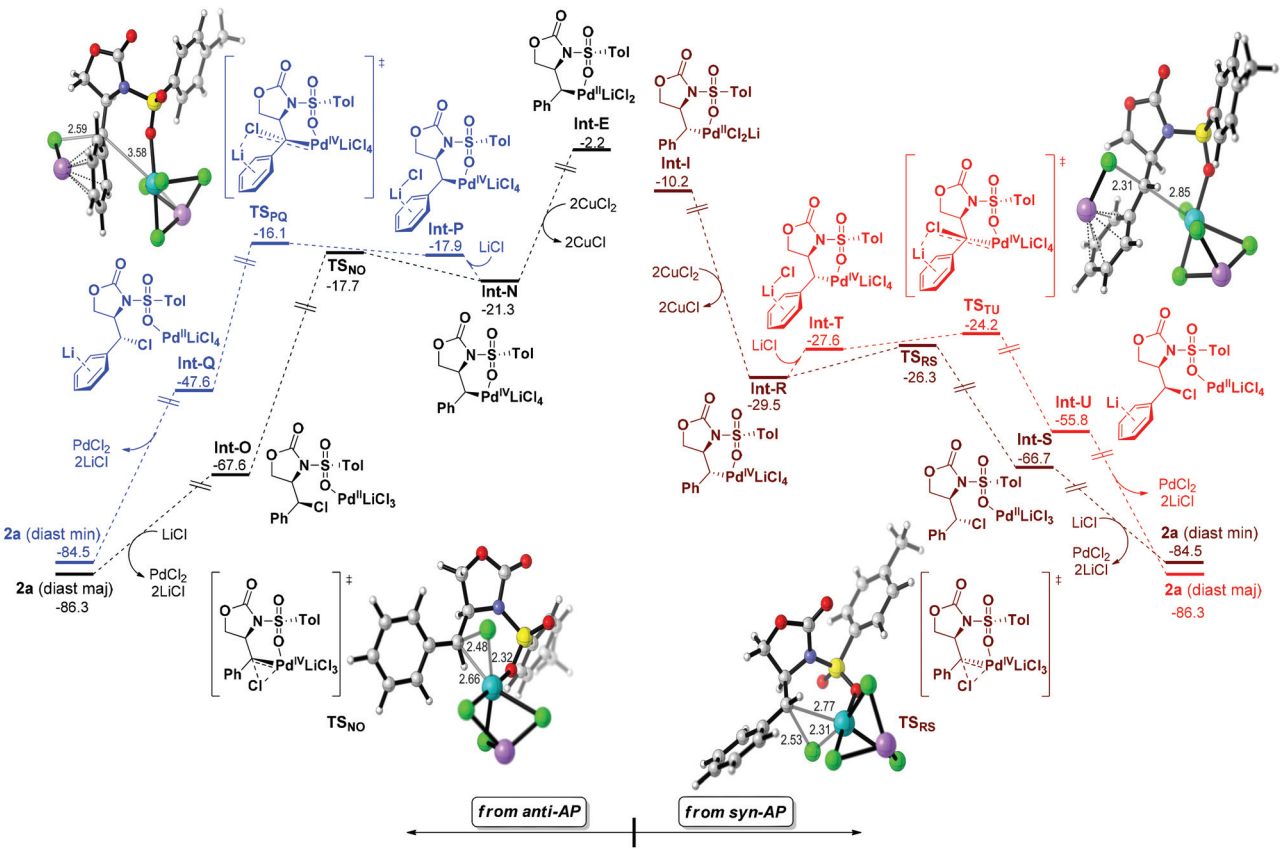

Fig. 5 Computed[31] free energy profiles for the C–Pd^{IV} oxidation followed by reductive elimination step *vs. anti*-S_N2-type chlorination–depalladation process to the formation of **2a** (both major and minor diastereomers). ΔG values in kcal mol^{-1} (acetonitrile, 333.15 K, 1 atm).

the catalyst. The intermediate **Int-N** could also be subject to an *anti*-S_N2-type chlorination-depalladation process due to the large excess of lithium chloride. Next, intermediate **Int-Q** is formed in a low $\mathbf{TS_{PQ}}$ barrier energy $\Delta G^{\ddagger}$ 1.8 kcal mol^{-1}, resulting in the minor diastereomer of **2a** by regenerating de palladium catalyst.

We also computationally investigated the formation of both diastereomers of **2a** from intermediate **Int-I** (formed through *syn*-AP path, see Fig. 3). Similar to formation of **Int-N**, intermediate **Int-I** is oxidized by $CuCl_2$ to give octahedral Pd(IV) complex **Int-R** (Fig. 5). Intermediate **Int-R** can also follow by: (i) direct formation of intermediate **Int-S** by reductive elimination from Pd(IV)-center *via* $\mathbf{TS_{RS}}$, forming the C–Cl bond with retention of the carbon configuration; or (ii) by association with lithium chloride intermediate **Int-T**, stabilized by Li–π interactions,[39] followed by an *anti*-S_N2-type chlorination-depalladation process to form intermediate **Int-U**, with both pathways depicting low energy barrier for $\mathbf{TS_{RS}}$ and $\mathbf{TS_{TU}}$ (Fig. 5). The latter step leads to concomitant depalladation of intermediates **Int-S** and **Int-U** and regenerates the palladium catalyst. In this way, we present an alternative mechanism that is energetically feasible for the formation of both diastereomers of **2a** obtained experimentally.

As described above, in addition to the regioselective formation of 5-membered rings, decarboxylative [3,3]-sigmatropic rearrangement by-products were also obtained. Previous studies have shown that allylic carbamates are excellent substrates for formal decarboxylative [3,3]-sigmatropic rearrangement palladium-catalyzed reactions.[13d,18b–c,40] The allylic amines obtained through [3,3]-sigmatropic rearrangement could justify the non-formation of a vicinal amino-chloro 6-membered ring. Based on the mechanism proposal to decarboxylative [3,3]-sigmatropic rearrangement of allylic carbamates described by Peters and collaborators,[18b–c] and mechanistic studies developed by Overman and collaborators[41] for allylic imidates, we calculated a pathway for the formation of allylic amine **3a** starting from a key-intermediate **Int-C** generated by *anti*-AP, which is a common intermediate for the 5-*endo*-closure (Fig. 6).

The intermediate **Int-C** is also subject to 6-*endo*-closure for the subsequent C–N bond formation that provides the cyclic σ-C–Pd bonded intermediate **Int-V**. This step occurs through endergonic transition state $\mathbf{TS_{CV}}$, which $\Delta\Delta G^{\ddagger}$ is 1.8 kcal mol^{-1} higher in energy than $\mathbf{TS_{CD}}$ responsible for 5-*endo*-closure *via* *anti*-AP (Fig. 6). In $\mathbf{TS_{CV}}$ transition structure, the formed cycle is in an envelope conformation with both palladium and phenyl ring substituents in pseudoequatorial positions. Intermediate **Int-V** undergoes ring-opening β-elimination along with decarboxylation to produce the amidate **Int-X** that after protonation and decomplexation furnish the allylic amine **3a** and regenerate the ammonium salt, lithium chloride and palladium(II) catalyst (Fig. 6).

Real time evaluation of intermediates

Mass spectrometric monitoring was performed with a Waters Acquity Triple Quadrupole Detector (TQD), in order to gain deeper insights about the mechanism of the amino-chloro-difunctionalization of allylic carbamates and unravel reaction intermediates, we evaluated the reaction mixture by direct injection ESI-MS/MS of the **1a** cyclization reaction media mediated by $PdCl_2(CH_3CN)_2$ for the formation of **2a**, as summarized in Fig. 7.[42–44]

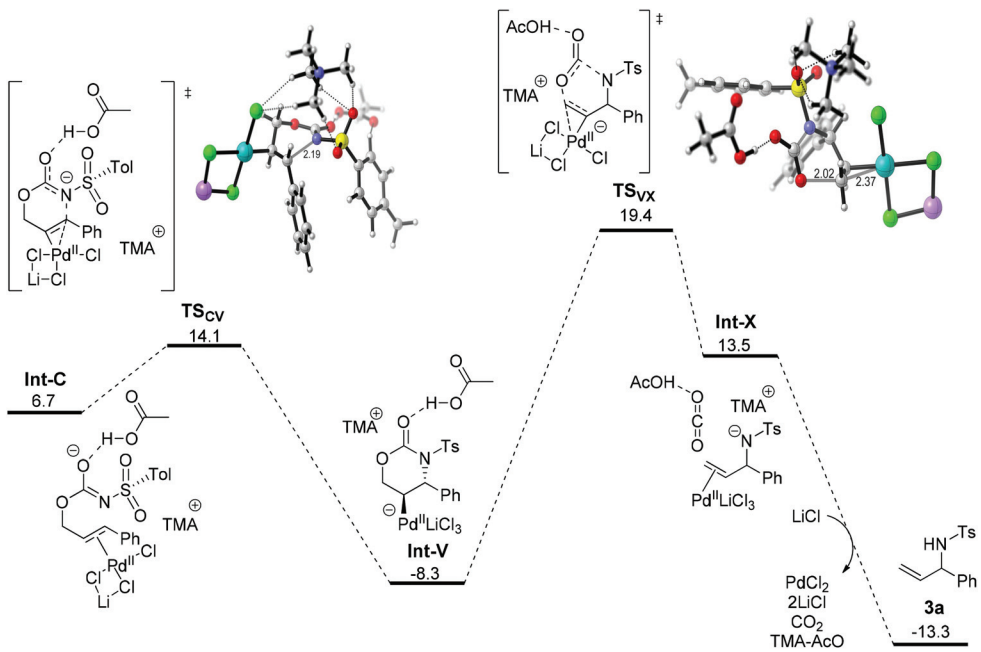

Fig. 6 Computed[31] free energy profiles for the decarboxylative formal [3,3]-rearrangement to the formation of **3a**. Δ*G* values in kcal mol^{-1} in relation to the isolated reactants (acetonitrile, 333.15 K, 1 atm).

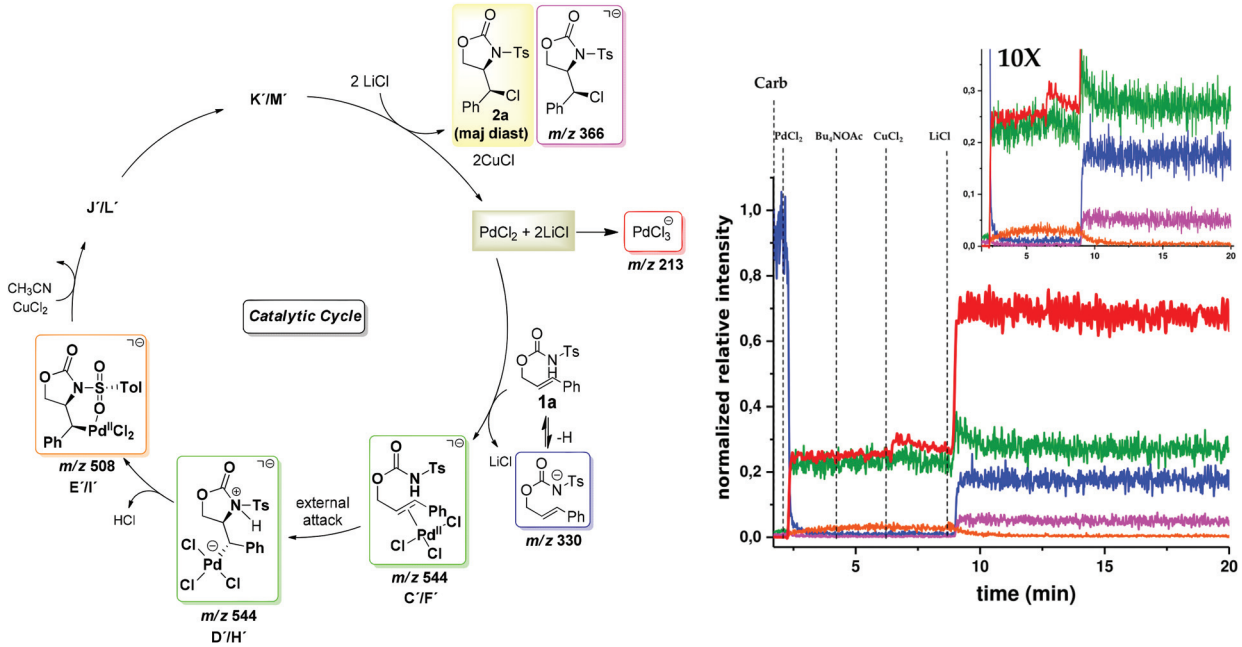

Fig. 7 Left – Simplified mechanism of **2a** formation from **1a** in presence of carbamate (**1a**, 0.02 mol L^{-1}, 1.0 mL) $PdCl_2(CH_3CN)_2$ (5.0 mol%), $CuCl_2$ (30 μmol L^{-1}, 1.0 mL) and LiCl (0.07 mol L^{-1}, 1.0 mL), Bu_4NOAc (20 nmol L^{-1}, 1.0 mL) in CH_3CN at 70 °C. Species highlighted in blue were observed by negative mode ESI-MS^2 (see text and ESI‡ for fragmentation patterns). Right – Evolution of ion intensity *vs.* reaction time. Dotted vertical lines indicate the time each component was added to the reaction media.

These results (Fig. 7 – left) show a simplified catalytic cycle based on the theoretical description reported above, highlighting the species proposed to take part in the mechanism as derived by the observed ions identified by mass spectrometry. The first step in the process is the coordination of carbamate **1a**, observed as the ion with *m/z* 330 in negative mode ESI,

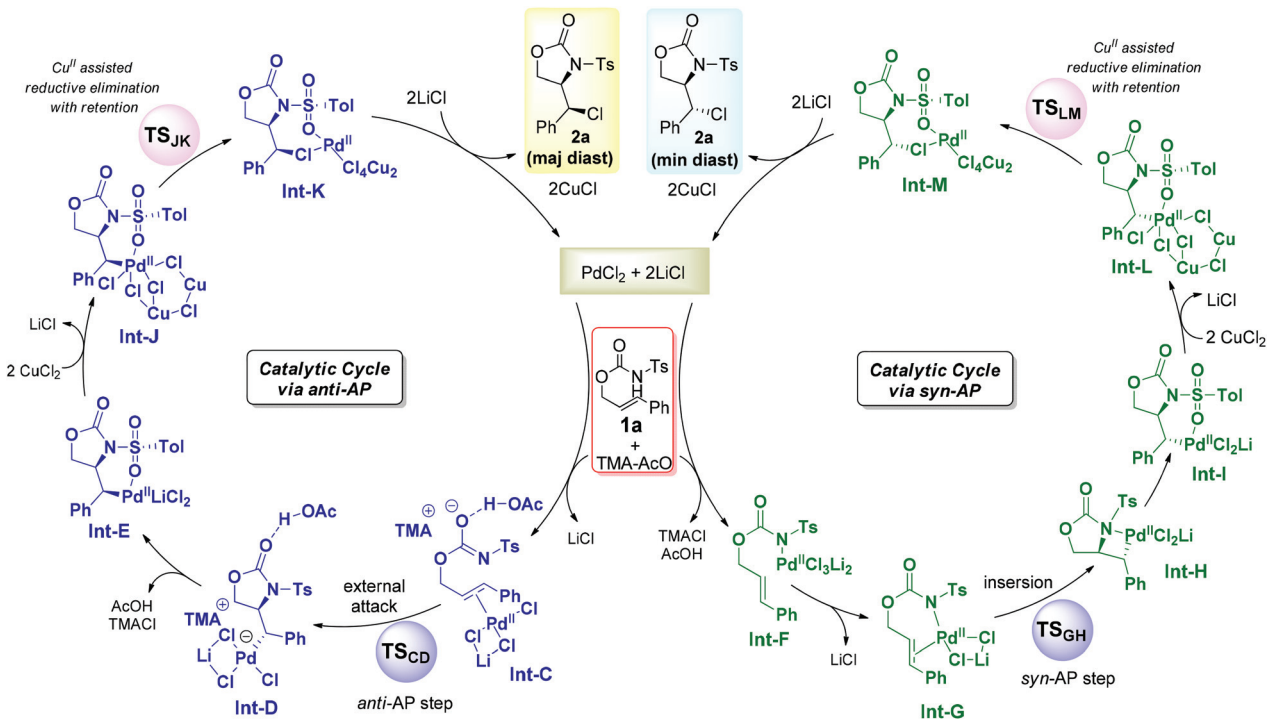

Scheme 6 Competitive catalytic cycles proposed for amino-chloro-difunctionalization of **1a**.

with the $PdCl_2$ to form either the species **Int-C** (*anti*-AP) or **Int-F** (*syn*-AP), as reported in Fig. 3. Upon the addition of $PdCl_2(CH_3CN)_2$ (Fig. 7 right), one can observe the immediate detection of $[PdCl_3]^-$, a reporter ion for the $PdCl_2$ complex, and formation of the species with *m*/*z* 544, assigned to the species **Int-C′**/**Int-F′** confirmed by MS^2 as well as the other ions reported, that may be correlated to the **Int-C**/**Int-F** species (Fig. 3), and to the isomer **Int-D′**/**Int-H′**, formed upon cyclization. It is also possible to observe the start of a slow formation of an ion with *m*/*z* 508, assigned to the species **Int-E′**/**Int-I′**, correlated with the initial species **Int-E**/**Int-I** of the chlorofunctionalization step.

Subsequent additions of Bu_4NOAc and $CuCl_2$ showed no significant change in the ion intensities, except for a small increment in the $[PdCl_3]^-$ intensity caused by the Cl^- addition to the system at 6 min (Fig. 7 right). The ion intensities responded only after the addition of LiCl. Nevertheless, control experiments showed that the reaction would only proceed if Bu_4NOAc and $CuCl_2$ were present in the reaction media before LiCl was added. The most significant change observed, besides the increase of $[PdCl_3]^-$ signal, was the slow decay of the intermediate **Int-E′**/**Int-I′** with *m*/*z* 508 and a compatible formation of the product **2a**, observed by the reporter ion **2a′** with *m*/*z* 366 (Fig. 7 – left). The LiCl addition also increased the deprotonated carbamate as the high chloride concentration may facilitate the formation of deprotonated carbamate.[45]

Consolidated mechanistic proposal

Based on our findings, Scheme 6 shows the overall proposed competitive catalytic cycles for the formation of **2a** (both major and minor diastereomer). These catalytic cycles suggest the two possible pathways for the aminopalladation, in which the *anti*-AP approach is responsible for the formation of major diastereomer and the *syn*-AP for the minor diastereomer, in agreement with theoretical and experimental results. Complementary, Cu(II) assists the installation of the second functionalization in which the carbon configuration is preserved, and the oxidation state of palladium remains in +2 throughout the process.

Conclusion

We have demonstrated the ability of simple Pd(II)-complexes to catalyze the vicinal diheterofunctionalization of internal alkenes, affording C_{sp^3}–N and C_{sp^3}–Cl bonds not typically generated by palladium-catalyzed processes. This cyclization reaction allows the rapid synthesis of a series of oxazolidinones in moderate to good yields with high to excellent diastereoselectivities from readily available precursors. The reaction is effective on a gram scale and was further applied to the synthesis of useful amino alcohols. We present in details a viable competitive mechanistic pathway for the formation of both diastereomers of the aminochlorocyclization supported by theoretical and experimental results. Our findings suggest the *anti*-aminopalladation mechanism followed by oxidative C–Pd(II) cleavage assisted by Cu(II) with retention of the carbon stereochemistry. Explorations toward an asymmetric variant of this transformation are currently underway in our laboratory.

Author contributions

B. P. Spadafora – conceptualization: supporting; investigation: lead; methodology: lead; visualization: equal; writing: original draft: supporting. F. W. M. Ribeiro – formal analysis: equal; investigation: equal; methodology: equal; visualization: equal; writing: original draft: supporting. J. E. Matsushima – investigation: supporting; validation: supporting; visualization: supporting. E. M. Ariga – investigation: supporting; validation: supporting. I. Omari – investigation: supporting; methodology: supporting; validation: supporting. P. M. A. Soares – methodology: supporting; validation: supporting. D. de Oliveira-Silva – investigation: supporting; supervision: supporting. E. Vinhato – conceptualization: equal; supervision: supporting; writing review & editing: equal. J. S. McIndoe – conceptualization: equal; funding acquisition: equal; supervision: equal; writing review & editing: equal. T. C. Correra – conceptualization: equal; funding acquisition: equal; supervision: equal; writing review & editing: equal. A Rodrigues – conceptualization: lead; formal analysis: lead; funding acquisition: lead; methodology: lead; project administration: lead; supervision: lead; writing review & editing: lead.

Conflicts of interest

There are no conflicts to declare.

Acknowledgements

We are grateful for financial support from Fundação de Amparo à Pesquisa do Estado de São Paulo – FAPESP (Grant: 2019/25634-9, 2016/21676-0, 2014/15962-5, 2015/08539-1, and scholarship to B. P. S. 2016/17328-7, and to F. W. M. R. 2019/16026-5, 2017/18485-1) and Coordenação de Aperfeiçoamento de Pessoal de Nível Superior – CAPES for scholarships to J. E. M., P. M. A. S. and E. M. A. and Grant 001 and 23038.006960/2014-65 to T. C. C. We also thank to Central Instrument Facility of UNIFESP. J. S. M. thanks the NSERC Discovery program for operational funding and CFI, BCKDF, and the University of Victoria for infrastructural support.

Notes and references

1 (*a*) A. Minatti and K. Muñiz, *Chem. Soc. Rev.*, 2007, **36**, 1142–1152; (*b*) R. I. McDonald, G. Liu and S. S. Stahl, *Chem. Rev.*, 2011, **111**, 2981–3019; (*c*) S. R. Chemler and D. A. Copeland, in *Top Heterocycl Chem*, 2013, pp. 39–75; (*d*) E. M. Beccalli, G. Broggini, S. Gazzola and A. Mazza,

Org. Biomol. Chem., 2014, **12**, 6767–6789; (*e*) P. Kočovský and J.-E. Bäckvall, *Chem. – Eur. J.*, 2015, **21**, 36–56; (*f*) G. Yin, X. Mu and G. Liu, *Acc. Chem. Res.*, 2016, **49**, 2413–2423; (*g*) M. M. Lorion, J. Oble and G. Poli, *Pure Appl. Chem.*, 2016, **88**, 381–389; (*h*) G. Broggini, T. Borelli, S. Giofré and A. Mazza, *Synthesis*, 2017, **49**, 2803–2818; (*i*) J. C. Hershberger, *Curr. Org. Chem.*, 2019, **23**, 1019–1044.

2 (*a*) E. J. Alexanian, C. Lee and E. J. Sorensen, *J. Am. Chem. Soc.*, 2005, **127**, 7690–7691; (*b*) D. Kalyani and M. S. Sanford, *J. Am. Chem. Soc.*, 2008, **130**, 2150–2151; (*c*) G. Yin and G. Liu, *Angew. Chem., Int. Ed.*, 2008, **47**, 5442–5445; (*d*) P. A. Sibbald, C. F. Rosewall, R. D. Swartz and F. E. Michael, *J. Am. Chem. Soc.*, 2009, **131**, 15945–15951; (*e*) A. J. Canty, *Dalton Trans.*, 2009, 10409–10417; (*f*) K. Muñiz, *Angew. Chem., Int. Ed.*, 2009, **48**, 9412–9423; (*g*) L.-M. Xu, B.-J. Li, Z. Yang and Z.-J. Shi, *Chem. Soc. Rev.*, 2010, **39**, 712–733; (*h*) C. Martínez and K. Muñiz, *Angew. Chem., Int. Ed.*, 2012, **51**, 7031–7034; (*i*) A. J. Hickman and M. S. Sanford, *Nature*, 2012, **484**, 177–185; (*j*) G. Yin, T. Wu and G. Liu, *Chem. – Eur. J.*, 2012, **18**, 451–455; (*k*) C. Martínez, Y. Wu, A. B. Weinstein, S. S. Stahl, G. Liu and K. Muñiz, *J. Org. Chem.*, 2013, **78**, 6309–6315; (*l*) P. Vinoth, M. Karuppasamy, B. S. Vachan, I. Muthukrishnan, C. U. Maheswari, S. Nagarajan, V. Pace, A. Roller, N. Bhuvanesh and V. Sridharan, *Org. Lett.*, 2019, **21**, 3465–3469.

3 (*a*) K. Muñiz, C. H. Hövelmann and J. Streuff, *J. Am. Chem. Soc.*, 2008, **130**, 763–773; (*b*) E. L. Ingalls, P. A. Sibbald, W. Kaminsky and F. E. Michael, *J. Am. Chem. Soc.*, 2013, **135**, 8854–8856; (*c*) K. H. Jensen, J. D. Webb and M. S. Sigman, *J. Am. Chem. Soc.*, 2010, **132**, 17471–17482.

4 H. Yu, Y. Fu, Q. Guo and Z. Lin, *Organometallics*, 2009, **28**, 4507–4512.

5 (*a*) X. Kou, Y. Li, L. Wu, X. Zhang, G. Yang and W. Zhang, *Org. Lett.*, 2015, **17**, 5566–5569; (*b*) X. Qi, C. Chen, C. Hou, L. Fu, P. Chen and G. Liu, *J. Am. Chem. Soc.*, 2018, **140**, 7415–7419; (*c*) H. Zhu, P. Chen and G. Liu, *Org. Lett.*, 2015, **17**, 1485–1488.

6 H. Zhu, P. Chen and G. Liu, *J. Am. Chem. Soc.*, 2014, **136**, 1766–1769.

7 (*a*) T. Wu, G. Yin and G. Liu, *J. Am. Chem. Soc.*, 2009, **131**, 16354–16355; (*b*) C. Hou, P. Chen and G. Liu, *Angew. Chem., Int. Ed.*, 2020, **59**, 2735–2739.

8 (*a*) C. Chen, P. Chen and G. Liu, *J. Am. Chem. Soc.*, 2015, **137**, 15648–15651; (*b*) C. Chen, C. Hou, P. Chen and G. Liu, *Chin. J. Chem.*, 2020, **38**, 346–350; (*c*) C. Chen, P. M. Pflüger, P. Chen and G. Liu, *Angew. Chem., Int. Ed.*, 2019, **58**, 2392–2396.

9 (*a*) D. Xing and D. Yang, *Org. Lett.*, 2013, **15**, 4370–4373; (*b*) L. Ye, K.-Y. Lo, Q. Gu and D. Yang, *Org. Lett.*, 2017, **19**, 308–311.

10 (*a*) Y. Tamaru, M. Hojo, H. Higashimura and Z. Yoshida, *J. Am. Chem. Soc.*, 1988, **110**, 3994–4002; (*b*) T. Shinohara, M. A. Arai, K. Wakita, T. Arai and H. Sasai, *Tetrahedron Lett.*, 2003, **44**, 711–714; (*c*) T. Tsujihara, T. Shinohara, K. Takenaka, S. Takizawa, K. Onitsuka, M. Hatanaka and H. Sasai, *J. Org. Chem.*, 2009, **74**, 9274–9279.

11 (*a*) P. A. Sibbald and F. E. Michael, *Org. Lett.*, 2009, **11**, 1147–1149; (*b*) G. Broggini, V. Barbera, E. M. Beccalli, U. Chiacchio, A. Fasana, S. Galli and S. Gazzola, *Adv. Synth. Catal.*, 2013, **355**, 1640–1648; (*c*) U. Chiacchio, G. Broggini, R. Romeo, S. Gazzola, M. A. Chiacchio, S. V. Giofrè, B. Gabriele, R. Mancuso, G. Floresta and C. Zagni, *RSC Adv.*, 2016, **6**, 57521–57529; (*d*) X. Liu, C. Hou, Y. Peng, P. Chen and G. Liu, *Org. Lett.*, 2020, **22**, 9371–9375; (*e*) X. Li, X. Qi, C. Hou, P. Chen and G. Liu, *Angew. Chem., Int. Ed.*, 2020, **59**, 17239–17244.

12 (*a*) M. R. Manzoni, T. P. Zabawa, D. Kasi and S. R. Chemler, *Organometallics*, 2004, **23**, 5618–5621; (*b*) J. Zhang, X. Wang, Y. Liu, X. Wang and W. He, *Appl. Organomet. Chem.*, 2017, **31**, e3631.

13 (*a*) A. Lei, X. Lu and G. Liu, *Tetrahedron Lett.*, 2004, **45**, 1785–1788; (*b*) P. Szolcsányi and T. Gracza, *Tetrahedron*, 2006, **62**, 8498–8502; (*c*) F. E. Michael, P. A. Sibbald and B. M. Cochran, *Org. Lett.*, 2008, **10**, 793–796; (*d*) S. D. R. Christie, A. D. Warrington and C. J. Lunniss, *Synthesis*, 2009, 148–154; (*e*) A.-D. Manick, F. Berhal and G. Prestat, *Synthesis*, 2016, **48**, 3719–3729; (*f*) J. Helaja and R. Göttlich, *Chem. Commun.*, 2002, **7**, 720–721.

14 T. Bach, B. Schlummer and K. Harms, *Chem. – Eur. J.*, 2001, **7**, 2581–2594.

15 C.-L. Zhu, J.-S. Tian, Z.-Y. Gu, G.-W. Xing and H. Xu, *Chem. Sci.*, 2015, **6**, 3044–3050.

16 S.-Q. Li, P. Xiong, L. Zhu, X.-Y. Qian and H.-C. Xu, *Eur. J. Org. Chem.*, 2016, 3449–3455.

17 For the reaction scheme for the synthesis of the starting materials, see Scheme S1 in the ESI.‡

18 (*a*) A. Joosten, A. K. Å. Persson, R. Millet, M. T. Johnson and J. E. Bäckvall, *Chem. – Eur. J.*, 2012, **18**, 15151–15157; (*b*) J. M. Bauer, W. Frey and R. Peters, *Angew. Chem., Int. Ed.*, 2014, **53**, 7634–7638; (*c*) J. M. Bauer, W. Frey and R. Peters, *Chem. – Eur. J.*, 2016, **22**, 5767–5777.

19 See ESI‡ for a more detailed screening of reaction conditions.

20 See ESI‡ for details on control experiments.

21 O. Gutierrez, J. G. Harrison, R. J. Felix, F. Cortés Guzman, M. R. Gagné and D. J. Tantillo, *Chem. Sci.*, 2013, **4**, 3894–3898.

22 (*a*) D. J. Ager, I. Prakash and D. R. Schaad, *Chem. Rev.*, 1996, **96**, 835–876; (*b*) S. C. Bergmeier, *Tetrahedron*, 2000, **56**, 2561–2576; (*c*) P. Gupta and N. Mahajan, *New J. Chem.*, 2018, **42**, 12296–12327.

23 H. Pan, H. Huang, W. Liu, H. Tian and Y. Shi, *Org. Lett.*, 2016, **18**, 896–899.

24 P. M. Henry, *J. Am. Chem. Soc.*, 1964, **86**, 3246–3250.

25 (*a*) J. E. Ney and J. P. Wolfe, *J. Am. Chem. Soc.*, 2005, **127**, 8644–8651; (*b*) L. S. Hegedus, G. F. Allen and E. L. Waterman, *J. Am. Chem. Soc.*, 1976, **98**, 2674–2676; (*c*) J. L. Brice, J. E. Harang, V. I. Timokhin, N. R. Anastasi and S. S. Stahl, *J. Am. Chem. Soc.*, 2005, **127**, 2868–2869; (*d*) G. Liu and S. S. Stahl, *J. Am. Chem. Soc.*, 2006, **128**,

7179–7181; (*e*) J. S. Nakhla, J. W. Kampf and J. P. Wolfe, *J. Am. Chem. Soc.*, 2006, **128**, 2893–2901; (*f*) J. E. Ney and J. P. Wolfe, *Angew. Chem., Int. Ed.*, 2004, **43**, 3605–3608; (*g*) X. Ye, G. Liu, B. V. Popp and S. S. Stahl, *J. Org. Chem.*, 2011, **76**, 1031–1044.

26 (*a*) U. Nettekoven and J. F. Hartwig, *J. Am. Chem. Soc.*, 2002, **124**, 1166–1167; (*b*) R. J. DeLuca, B. J. Stokes and M. S. Sigman, *Pure Appl. Chem.*, 2014, **86**, 395–408; (*c*) I. Franzoni, L. Guénée and C. Mazet, *Org. Biomol. Chem.*, 2015, **13**, 6338–6343.

27 T. Hosokawa, M. Takano and S.-I. Murahashi, *J. Am. Chem. Soc.*, 1996, **118**, 3990–3991.

28 A. K. El-Qisairi, H. A. Qaseer, G. Katsigras, P. Lorenzi, U. Trivedi, S. Tracz, A. Hartman, J. A. Miller and P. M. Henry, *Org. Lett.*, 2003, **5**, 439–441.

29 G. Savitha, K. Felix and P. Perumal, *Synlett*, 2009, 2079–2082.

30 X. Wan, Z. Ma, B. Li, K. Zhang, S. Cao, S. Zhang and Z. Shi, *J. Am. Chem. Soc.*, 2006, **128**, 7416–7417.

31 All calculations were carried out with Gaussian09 at the M06-2X/Def2-TZVPP(Pd,Cu)/6-311++g(2df,2pd)(all others)//PBE1PBE/Def2-TZVPP(Pd,Cu)/6-31 g(d,p)(all others)/SMD level in acetonitrile (for full citation and computational details, see ESI‡).

32 G. N. Babu, A. R. B. Rao, S. Keesara and S. Pal, *J. Organomet. Chem.*, 2017, **848**, 243–248.

33 (*a*) L. D. Taylor, R. J. MacDonald and L. E. Rubin, *J. Polym. Sci., Part A-1: Polym. Chem.*, 1971, **9**, 3059–3061; (*b*) P. Unsworth, L. Löffler, A. Noble and V. Aggarwal, *Synlett*, 2015, **26**, 1567–1572.

34 J.-E. Bäckvall, B. Åkermark and S. O. Ljunggren, *J. Chem. Soc., Chem. Commun.*, 1977, 264–265.

35 (*a*) O. Hamed, C. Thompson and P. M. Henry, *J. Org. Chem.*, 1997, **62**, 7082–7083; (*b*) O. Hamed and P. M. Henry, *Organometallics*, 1997, **16**, 4903–4909; (*c*) O. Hamed, P. M. Henry and C. Thompson, *J. Org. Chem.*, 1999, **64**, 7745–7750.

36 (*a*) J. A. Keith, R. J. Nielsen, J. Oxgaard and W. A. Goddard, *J. Am. Chem. Soc.*, 2007, **129**, 12342–12343; (*b*) J. A. Keith, R. J. Nielsen, J. Oxgaard, W. A. Goddard and P. M. Henry, *Organometallics*, 2009, **28**, 1618–1619.

37 (*a*) T. Hosokawa, T. Nomura and S.-I. Murahashi, *J. Organomet. Chem.*, 1998, **551**, 387–389; (*b*) Y. Kawamura, Y. Kawano, T. Matsuda, Y. Ishitobi and T. Hosokawa, *J. Org. Chem.*, 2009, **74**, 3048–3053.

38 (*a*) G. Zhu, S. Ma, X. Lu and Q. Huang, *J. Chem. Soc., Chem. Commun.*, 1995, **12**, 271–273; (*b*) G. Zhu and X. Lu, *J. Organomet. Chem.*, 1996, **508**, 83–90.

39 D. A. Dougherty, *Acc. Chem. Res.*, 2013, **46**, 885–893.

40 (*a*) A. Lei and X. Lu, *Org. Lett.*, 2000, **2**, 2357–2360; (*b*) M. Agirre, S. Henrion, I. Rivilla, J. I. Miranda, F. P. Cossío, B. Carboni, J. M. Villalgordo and F. Carreaux, *J. Org. Chem.*, 2018, **83**, 14861–14881.

41 M. P. Watson, L. E. Overman and R. G. Bergman, *J. Am. Chem. Soc.*, 2007, **129**, 5031–5044.

42 A. Joshi, H. S. Zijlstra, S. Collins and J. S. McIndoe, *ACS Catal.*, 2020, 7195–7206.

43 L. P. E. Yunker, Z. Ahmadi, J. R. Logan, W. Wu, T. Li, A. Martindale, A. G. Oliver and J. S. McIndoe, *Organometallics*, 2018, **37**, 4297–4308.

44 R. G. Belli, Y. Wu, H. Ji, A. Joshi, L. P. E. Yunker, J. S. McIndoe and L. Rosenberg, *Inorg. Chem.*, 2019, **58**, 747–755.

45 P. Kebarle and U. H. Verkerk, *Mass Spectrom. Rev.*, 2009, **28**, 898–917.

